Insight on the Natural Moroccan Clay Valorization for Malachite Green Adsorption: Kinetic and Isotherm Studies

Hassan OUALLAL[1,a,*], Mohammed CHRACHMY[1,b], Najia EL HAMZAOUI[2,c],
Mahdi LECHHEB[1,d], Rajae GHIBATE[3,e], Houssam EL-MARJAOUI[4,f],
and Mohamed AZROUR[1,g]

[1]Laboratory of Materials Engineering for the Environment and Natural Resources, Faculty of Science and Technology, Moulay Ismail University, Errachidia, 52000, Morocco

[2]Laboratory of Ecology and Biodiversity of Wetlands, Faculty of Sciences, Moulay Ismail University, Meknes, 11201, Morocco

[3]Laboratory of Physical Chemistry, Materials, and Environment, Faculty of Sciences and Technologies, Moulay Ismail University, Errachidia, 52000, Morocco

[4]Laboratoire de Spectrométrie des Matériaux et Archéomatériaux (LASMAR), Unité de Recherche Labéllisée par CNRST (URL-CNRST N°7), Université Moulay Ismail, Faculté des Sciences, Zitoune BP 11201, 50000 Meknès, Morocco

[a]hassanouallalaghbalou@gmail.com, [b]mo.chrachmy@edu.umi.ac.ma,
[c]najia.elhamzaoui@gmail.com, [d]m.lechheb@edu.umi.ac.ma, [e]rajae.ghibate@gmail.com,
[f]elmarjaoui1993@gmail.com, [g]m.azrour@fste.umi.ac.ma

Keywords: Natural Clay, Adsorption, Malachite Green, Kinetic Modeling, Isotherm Study

Abstract. This work investigates the potential of Natural Moroccan Clay (NMC) sourced from the Draa-Tafilalet region for removing malachite green from aqueous media through adsorption. X-ray diffraction (XRD) and scanning electron microscopy combined with energy-dispersive X-ray microanalysis (SEM/EDX) were used to characterize the clay. Malachite green (MG) was subjected to batch adsorption experiments, and a kinetic study was carried out at three concentrations (5, 50, and 100 mg/L). The results showed that adsorption is typically fast for all three concentrations and that the adsorbed amount rises with time and dye concentration. Equilibrium is reached within just 40 minutes. The kinetics adsorption at varying MG concentrations were modeled using non-linear and linear forms of pseudo-first order and pseudo-second order and with intraparticle diffusion models. The non-linear form of the pseudo-second-order model was found to be best suited to describing this adsorption process. The isotherm was studied using two models: Freundlich and Langmuir. According to the error functions analysis, the Langmuir model is well suited for equilibrium data fitting. Investigated clay attained an adsorption capacity of 214 mg/g. SEM/EDX characterization of NMC before and after adsorption confirms the malachite green adsorption on the NMC surface. These results illustrate the effectiveness of the investigated clay as a cost-effective adsorbent.

Introduction

Nowadays, water vulnerability is heightened by climate change and the expansion of the industrial world, increasing volumes of effluent discharged into the natural medium. That is detrimental to the environment and, by extension, to public health [1,2]. Among the pollutants present in these effluents are dyes. The present study focuses on the remediation of water contaminated with malachite green (MG), one of the dyes recognized for its mutagenic and carcinogenic effects on living beings, once released into the environment [1,3]. Several treatment technologies have been proposed for MG removal by other researchers, including advanced oxidation processes [4], membrane separation [5], and adsorption [6]. In this context, clays have found a way to be used as

an adsorbent, given their particular physico-chemical characteristics, abundance, and low cost. Indeed, some clay materials have demonstrated excellent adsorption capacity, high surface reactivity, and notable cation exchange potential [7,8].

This study aims to valorize natural Moroccan clay (NMC) from the Es-sifa commune in the Draa-Tafilalet region as an adsorbent for treating water containing MG dye. The clay studied was characterized by SEM/EDX and XRD. Furthermore, kinetic and isotherm studies were conducted to understand better the reaction mechanism of MG fixation on the NMC surface. The adequacy of the investigated models was ensured and evaluated by error functions.

Materials and Methods

Adsorbate

Malachite green oxalate ($C_{52}H_{54}N_4O_{12}$) was supplied by VWR Chemicals. Fig. 1 illustrates its chemical structure. A precisely weighed mass of dye powder is dissolved in demineralized water to prepare a dye stock solution. Different concentrations were prepared from this solution.
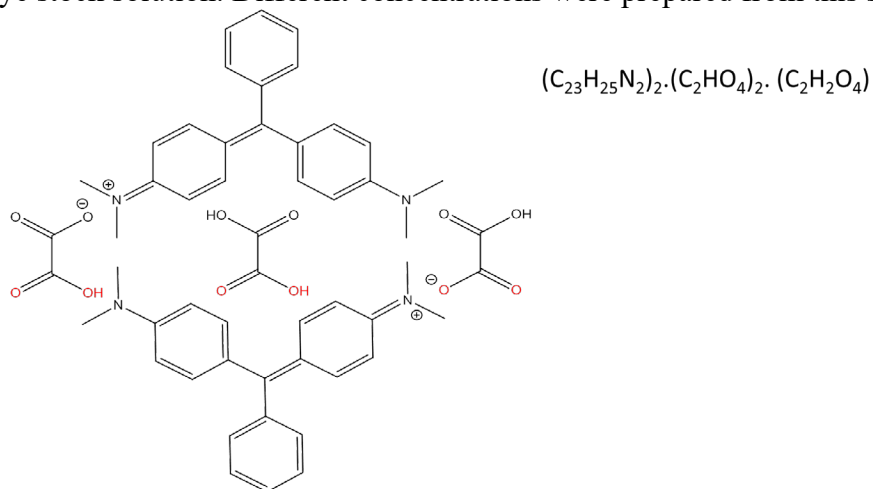

$(C_{23}H_{25}N_2)_2 \cdot (C_2HO_4)_2 \cdot (C_2H_2O_4)$

Figure 1: Malachite green oxalate chemical structure

Clay preparation

The NMC used in the adsorption experiments was collected from Es-sifa, located in the province of Errachidia, Morocco. The natural clay was crushed and passed through ISO standard mesh sieves, and only particles smaller than 315 μm were utilized for the experiments.

Clay Characterization

The NMC was characterized using XRD and SEM/EDX. The NMC mineralogy was analyzed by X-ray powder diffraction. The XRD pattern was obtained using an X'Pert PRO MPD diffractometer instrument with a wavelength of 1.5406 Å of CuKα radiation. The scanning of the 2θ angle was conducted within the range of 10 to 30 with an increment of 0.02 for 2 seconds.
The morphology of NMC was examined using SEM/EDX analysis (JSM-IT500HR) at 10 kV acceleration voltage under room temperature. NMC sample after MG adsorption was first metalized and fixed to carbon support before being analyzed.

Adsorption experiments

The experiments of adsorption were executed in batch mode to determine equilibrium time and observe the influence of time on MG. In each experiment, 100 mg of NMC was introduced into 100 mL of solutions with varying MG concentrations (5, 50, and 100 mg/L). These mixtures were maintained at different contact times (5 to 60 min) and underwent agitation at 250 revolutions per minute at a temperature of 25 C. For the isotherm study, experiments were conducted at 25 °C with varying concentrations from 5 to 300 mg/L.

For every test, 100 mL of the MG solution was mixed with 100 mg of clay. These mixtures were immediately shaken at 250 rpm for 60 minutes. Following each experiment, the mixture is filtered, and the residual dye concentration is measured with a Shimadzu UV-160 UV/Visible spectrometer at 620 nm. According to the equation below, the adsorbed quantity was calculated:

$$q_t = \frac{C_0 - C_t}{m_{clay}} \times V_{MG} \tag{1}$$

Where
m_{clay}: mass of clay (g)
V_{MG}: volume of malachite green solution (L)
C_0: initial concentrations of MG
C_t: concentrations of MG at t time (M)
q_t: adsorption quantity at t time (mg/g)

Kinetic modeling
The kinetic data was fitted with non-linear and linear equations of the pseudo-first-order model (PFOM) and pseudo-second-order model (PSOM), along with the model of intraparticle diffusion (PDM). This was done to find out how malachite green was adsorbed onto the studied clay. The table below outlines these models.

Table 1: kinetic models of adsorption

Model	Non-linear equation	Linear equation	Parameters	Reference
Pseudo-first order	$q_t = q_e(1 - e^{-K_1 t})$	$ln(q_e - q_t) = ln(q_e) - K_1 t$	K_1	[9]
Pseudo-second order	$q_t = \frac{q_e^2 K_2 t}{q_e K_2 t + 1}$	$\frac{t}{q_t} = \frac{1}{q_e^2 K_2} + \frac{1}{q_e}t$	K_2	[9]
Intraparticle diffusion	–	$q_t = K_{id} t^{1/2} + C_i$	K_{id}, C_i	[10]

q_e (mg/g) represents the equilibrium adsorption quantity. C is the thickness of boundary layer. K_1 (min^{-1}), K_2 (min.g/mg), and K_{id} (mg/g.min$^{1/2}$) correspond to the adsorption rate constants of the PFOM, PSOM, and IPDM, respectively.

Equilibrium Isotherm Modeling
For the isotherm study, solutions of MG with varying concentrations (5 - 300 mg/L). The dye adsorption was carried out under optimized conditions of 0.10 g of adsorbent mass, agitation speed of 250 rpm, and pH of the medium. The finding was plotted with Langmuir and Freundlich models. The relevant parameters were calculated from the non-linear plots using equations below:

$$q_e = \frac{q_{max} K_L C_e}{1 + K_L C_e} \tag{2}$$

$$q_e = K_F C_e^{1/n} \tag{3}$$

C_e (mg/L) stands for the dye concentration that is still present at equilibrium. q_{max} (mg/g) represents the maximum adsorption capacity. The Langmuir constant is designated by K_L (L/mg). The K_F ((mg/g)(mg/L)$^{-1/n}$) and n stand for the constants of Freundlich.

Error analysis

The adaptation of the models was deemed through error function analysis, which included the standard deviation (Δq (%)), Chi-square (χ^2), and the coefficient of determination (R^2) [11,12]

$$\Delta q(\%) = 100 \times \left\{ \frac{\sum_{i=1}^{n} \left[(q_{exp} - q_{cal}) / q_{exp} \right]^2}{n-1} \right\}^{1/2} \tag{5}$$

$$\chi^2 = \sum_{i=1}^{n} \frac{(q_{exp} - q_{cal})^2}{q_{cal}} \tag{6}$$

$$R^2 = \frac{\sum_{i=1}^{n} (q_{cal} - \overline{q_{exp}})^2}{\sum_{i=1}^{n} (q_{cal} - \overline{q_{exp}})^2 + \sum_{i=1}^{n} (q_{cal} - q_{exp})^2} \tag{4}$$

Results and Discussion

Clay characterization

Fig. 2 displays the diffractogram of NMC, revealing the existence of various mineral phases. These encompass silica in the form of quartz (Q), kaolinite (K), dolomite (D), and calcite (C) [13–16].
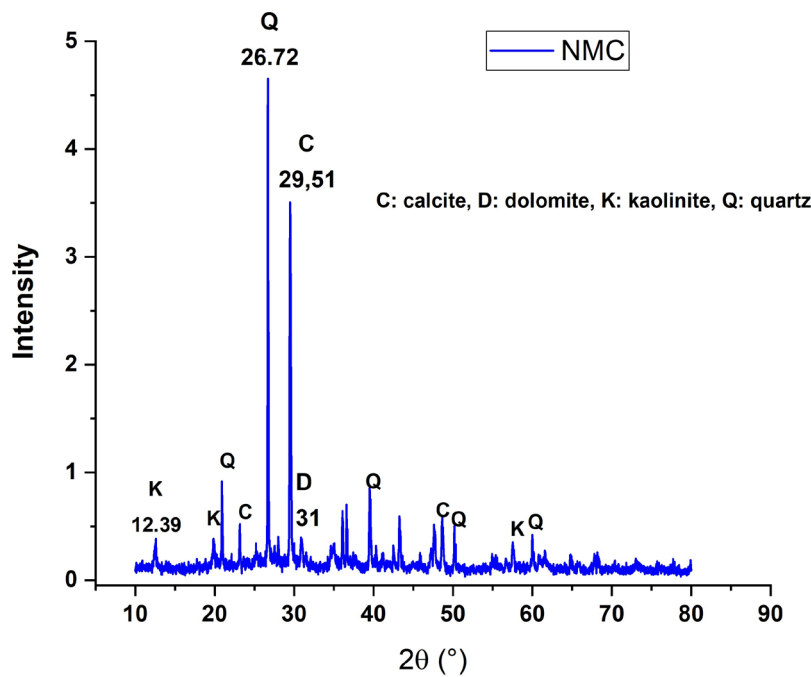

Figure 2: XRD pattern of NMC

Kinetic study

The malachite green adsorption onto NMC was studied to determine if equilibrium had been reached. The adsorption was conducted at different concentrations (5, 50, and 100 mg/L) in a time-dependent study (Fig.3). The findings showed that the adsorption of MG on NMC occurred rapidly within the first few minutes of contact at all three concentrations. However, as time progressed, adsorption became slower. Equilibrium was reached at 40 minutes. A possible explanation for this is the abundance of active sites on the surface of the NMC, which gradually demineralize until they become saturated. The quantity adsorbed rises with the adsorbate concentration, according to

an analysis of kinetic data. That makes sense since the concentration gradient is getting steeper, which encourages the dye to diffuse toward the adsorbent.[17]
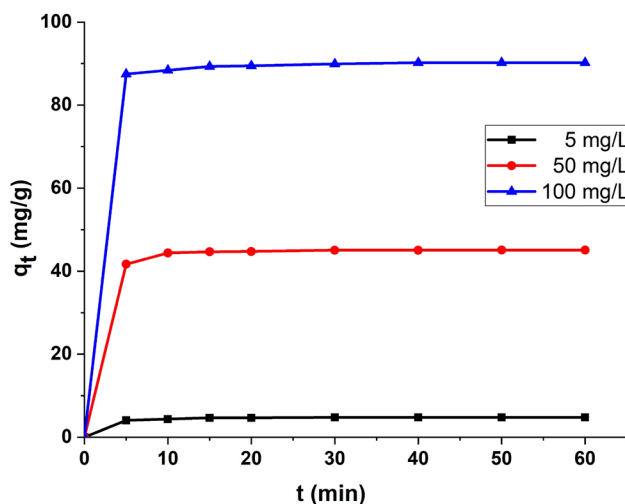

Figure 3: Kinetic of MG adsorption onto NMC at different dye concentrations

The kinetics of MG adsorption by raw clay were modeled using both linear and nonlinear forms of PFOM and PSOM as illustrated in Figs. 4 and 5. Table 2 displays the parameters for these models. The findings indicate that there is a weak correlation between the linear and nonlinear forms of the PFOM. Therefore, MG adsorption onto NMC does not follow PFOM kinetics. However, two forms of the PSOM showed correlation coefficient values (R^2) close to unity, revealing the best fit of this model to the MG adsorption kinetic. Furthermore, the predicted equilibrium amounts of MG adsorbed with the nonlinear form of the PSOM are very close to those measured experimentally, which is well supported by the low values of Δq and $\chi 2$. Accordingly, this form provides a better description of MG adsorption on NMC.
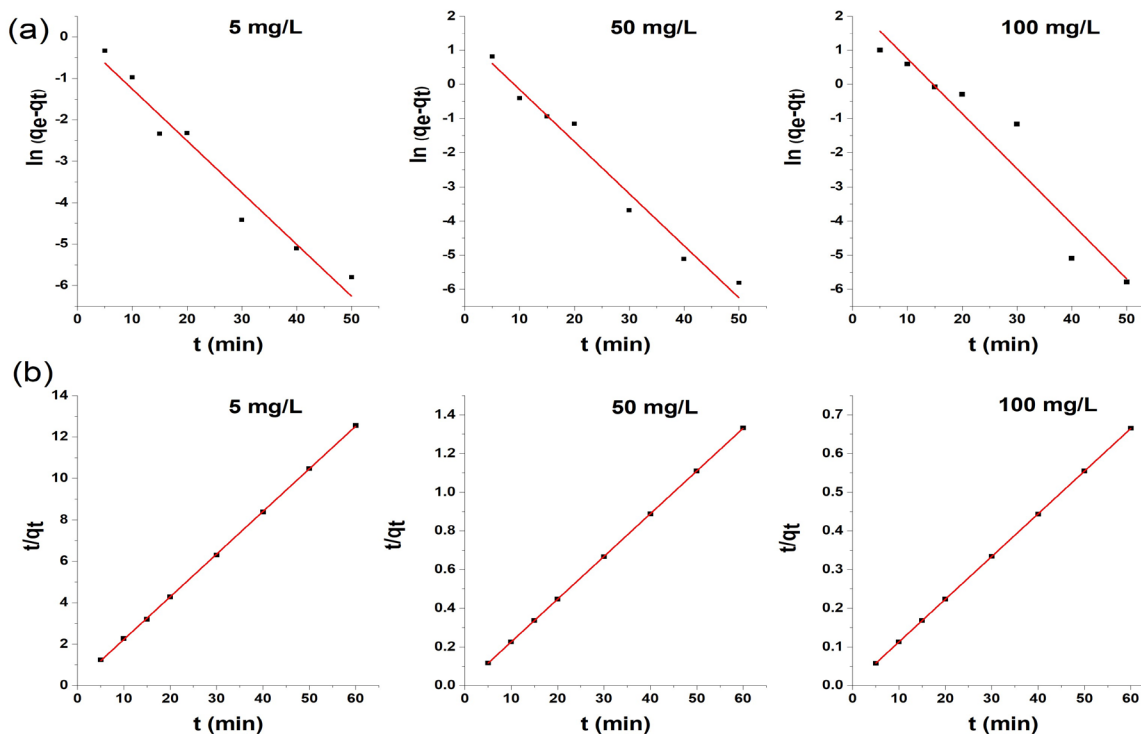

Figure 4: The plots of the linear form of PFOM (a) and PSOM (b) at different MG concentrations
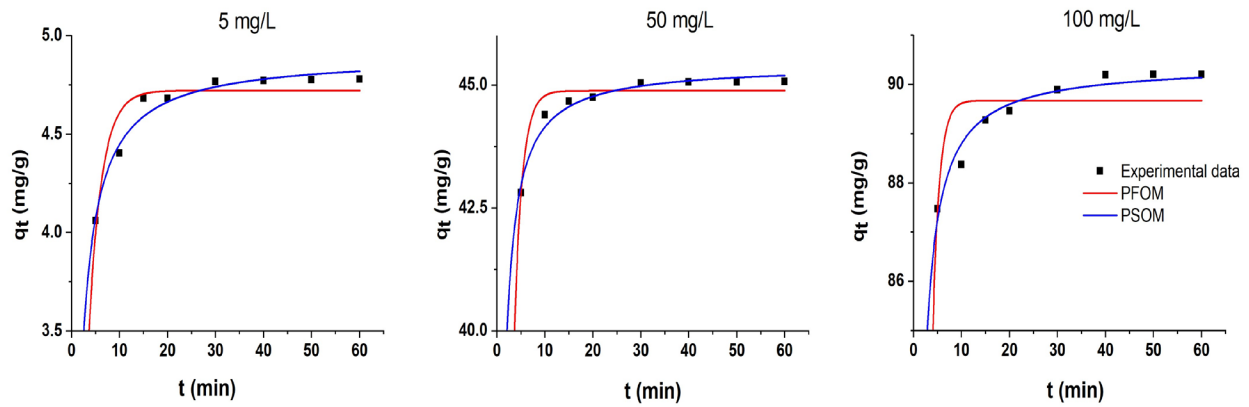
Figure 5: The plots of the nonlinear form of PFOM and PSOM at different MG concentrations

Table 2: PFOM and PSOM kinetic parameters at different MG concentrations using linear and non-linear forms.

MG concentration	Parameter & statistical error	PFOM		PSOM	
		LF	NLF	LF	NLF
5 mg/L	$q_{e, cal}$(mg/g)	0.99	4.72	4.86	4.90
	K_1 (min^{-1}) / K_2 (min.g.mg^{-1})	0.1250	0.3740	0.2579	0.2006
	R^2	0.9599	0.9969	0.9999	0.9993
	χ^2	124.26	0.0130	0.0073	0.0031
	Δq (%)	88.54	2.08	1.59	0.97
50 mg/L	$q_{e, cal}$(mg/g)	3.96	44.88	45.27	45.41
	K_1 (min^{-1}) / K_2 (min.g.mg^{-1})	0.1526	0.6111	0.1023	0.0772
	R^2	0.9753	0.9998	1.0000	0.9999
	χ^2	3 537.2	0.0075	0.0084	0.0028
	Δq (%)	99.60	0.49	0.54	0.30
100 mg/L	$q_{e, cal}$(mg/g)	10.7423	89.6762	90.5797	90.4141
	K_1 (min^{-1}) / K_2 (min.g.mg^{-1})	0.1614	0.7360	0.0512	0.0610
	R^2	0.9257	0.9996	1.0000	1.0000
	χ^2	4 875.4	0.0293	0.0061	0.0035
	Δq (%)	96.51	0.69	0.32	0.24

Fig. 6 shows multi-linear intraparticulaire diffusion plots, which do not cross the origin, suggesting that other rate-step processes control the MG adsorption for the three concentrations than intraparticle diffusion. The steeply sloping initial linear section reflects external mass transfer, the second half shows intraparticle diffusion, and the plateau region represents equilibrium [10]

Therefore, the boundary layer thickness (C) and the rate constant of the intraparticle diffusion (K_{id}) were generated from the intercept and the slope of the middle linear section (Table 3).[18]
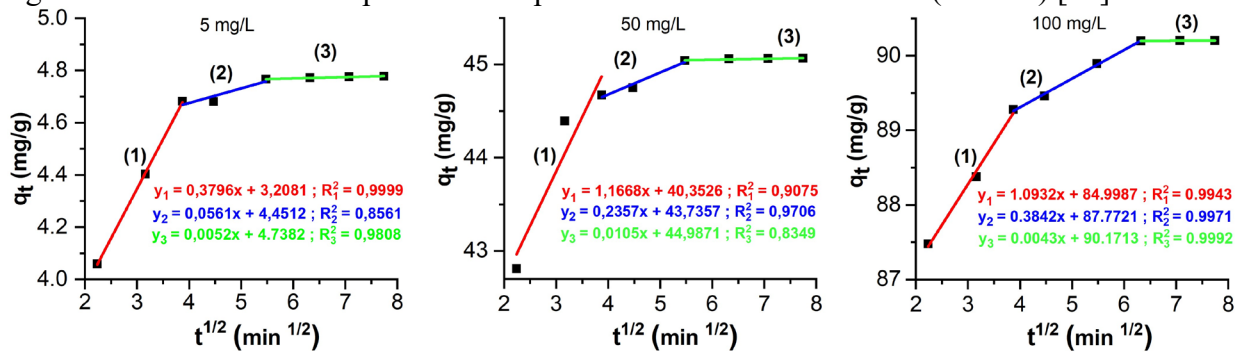

Figure 6: Intraparticulaire diffusion plots of MG adsorption onto NMC at different concentrations

Table 3: Kinetic parameters from the intraparticulaire diffusion at different MG concentrations

Step	Parameter	Concentration (mg/L)		
		5	**50**	**100**
First step	$K_{id,1}$ (mg/g.min$^{1/2}$)	0.3796	1.1668	1.0932
	C_1	3.2081	40.3526	84.9987
	R^2	0.9999	0.9075	0.9943
Second step	$K_{id,2}$ (mg/g.min$^{1/2}$)	0.0561	0.2357	0.3842
	C_2	4.4512	43.7357	87.7721
	R^2	0.8561	0.9706	0.9971
Third step	$K_{id,3}$ (mg/g.min$^{1/2}$)	0.0052	0.0105	0.0043
	C_3	4.7382	44.9871	90.1713
	R^2	0.9808	0.8349	0.9992

Isotherm study

Fig. 7 shows the experimental results of the isotherm study, with their predictions by the nonlinear forms of the Freundlich and Langmuir models. Table 4 summarizes the results of this study. Analysis of the error functions R^2, Δq, and χ^2 clearly shows that Langmuir model most appropriate for describing the MG adsorption isotherm on the clay studied. That suggests that MG is adsorbed as a monolayer on energetically comparable sites without any interaction between the adsorbed MG molecules[19]. The maximum adsorption quantity predicted by this model is 245.67 mg/g.

Table 4: Freundlich and Langmuir isotherm constants and their error analysis

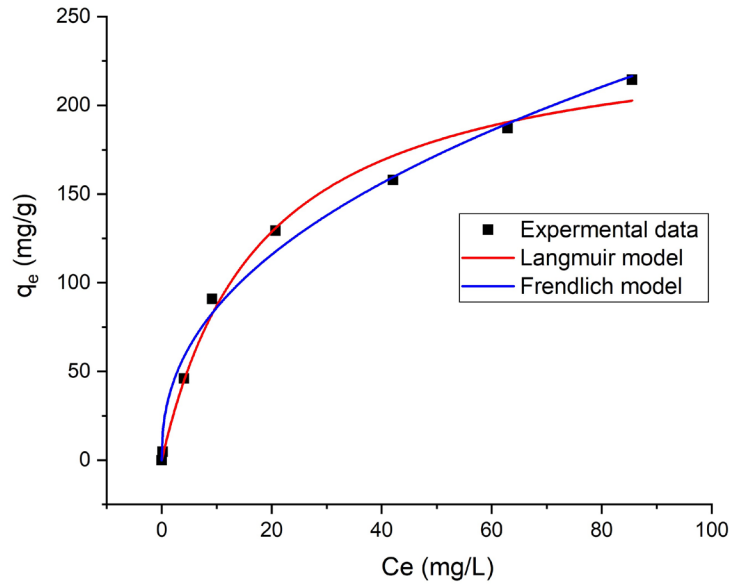| $q_{max, exp}$ (mg/g)	Langmuir						Freundlich					
	$q_{max, cal}$ (mg/g)	K_L (L/mg)	R^2	χ^2	Δq (%)		$q_{max, cal}$ (mg/g)	K_F (mg/g)	$1/n$	R^2	χ^2	Δq (%)
214.51	245.67	0.05	0.9911	0.92	21.94		216.51	31.87	0.43	0.9901	11.45	86.91

Figure 7: Adsorption isotherm of MG at 25°C and their fitting through Freundlich and Langmuir models

The dimensionless constant R_L is an essential characteristic of the Langmuir isotherm calculated using K_L and C_0 as per the following equation:

$$R_L = \frac{1}{1 + K_L C_0} \tag{7}$$

The adsorption procedure can be categorized depending on the R_L value. It's favorable if the R_L value is between 0 and 1, linear if R_L is around 1, irreversible if R_L is zero, and unfavorable if R_L is greater than 1[20].

Fig. 8 illustrates how R_L changes with the initial concentration. As the figure depicts, the R_L values range from 0 to 1, indicating a favorable MG adsorption process onto NMC.
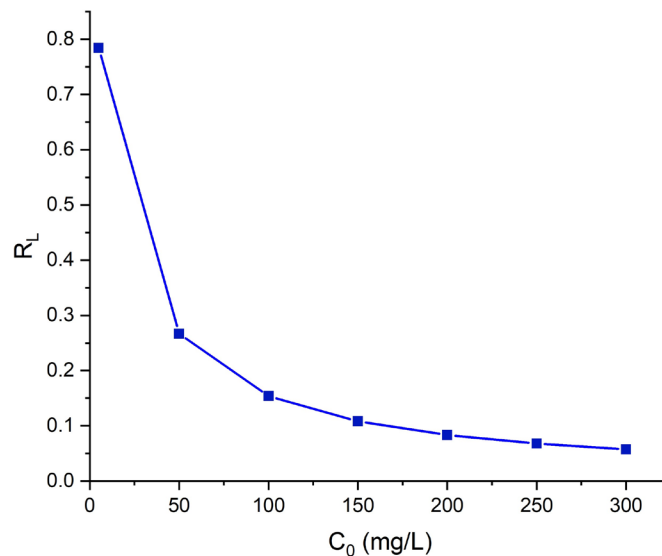

Figure 8: The plot of the R_L values as a function of concentration for MG adsorption onto NMC

ESM/EDX characterization

In Fig. 9, the scanning electron microscope images show a clear difference in the surface appearance of the adsorbent before and after adsorption. The surface of the clay is now covered with malachite green molecules, as confirmed by the comparison of the EDX spectra of NMC before and after adsorption. The spectra analysis revealed an increase in carbon intensity, with the percentage of carbon rising from 7.6% to 23%. This increase could be attributed to the organic nature of the malachite green dye, which has bonded to the clay surface.
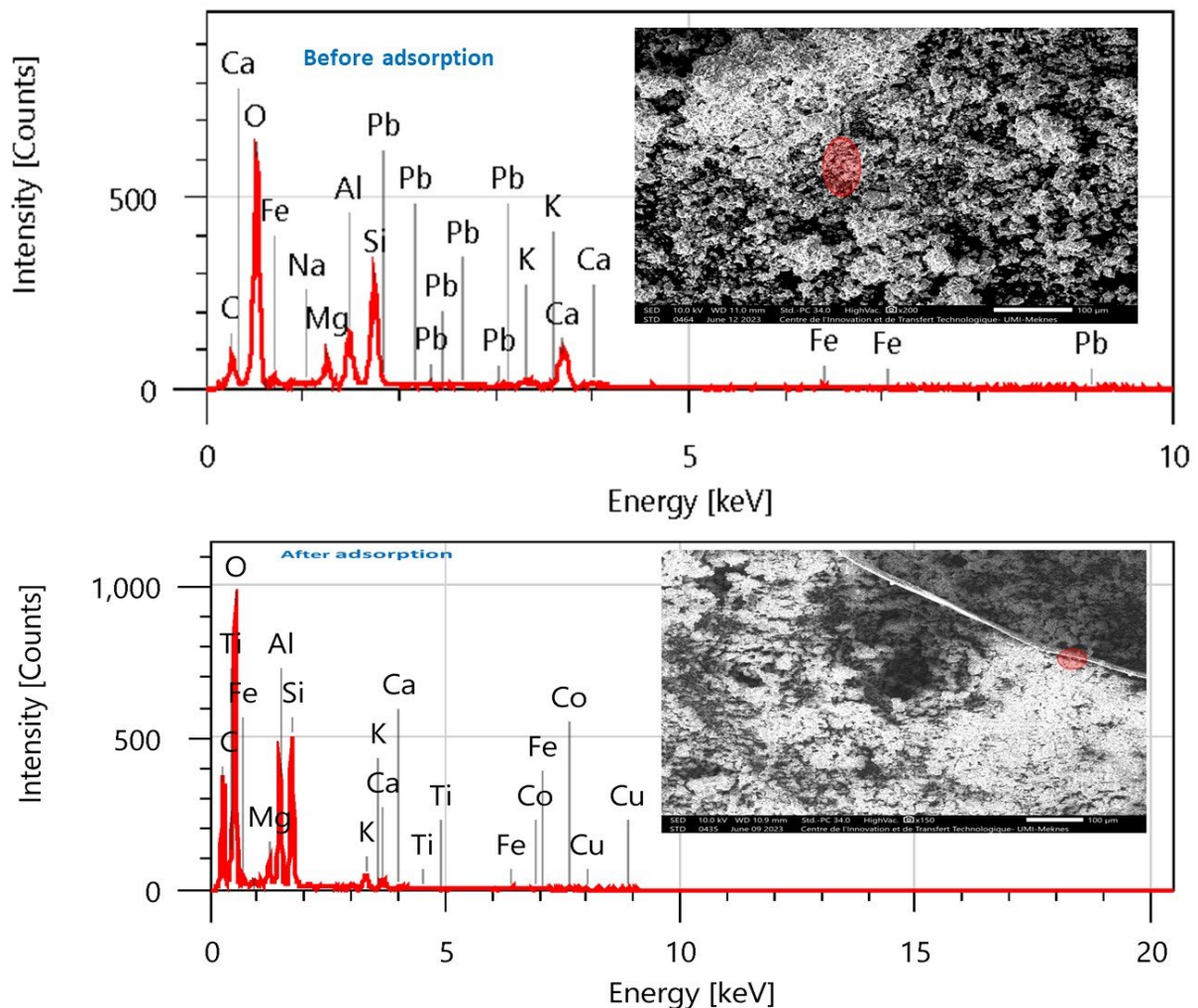

Figure 9: SEM images and EDX spectra of NMC before and after MG adsorption

Conclusion

This study investigates the effectiveness of natural Moroccan clay from the Draa-Tafilalet region in removing malachite green from aqueous solutions. XDR analysis revealed that the clay predominantly consists of kaolinite, calcite, dolomite, and quartz. The findings suggest a favorable adsorption potential for malachite green dye. As the concentration increases from 5 to 100 mg/L, the adsorption quantity escalates from 4.78 to 90.20 mg/g. The kinetics of adsorption align precisely with the pseudo-second-order model. Additionally, it was observed that intraparticle diffusion does not singularly govern the process. The Langmuir model proves most apt for fitting equilibrium data, revealing a maximum adsorption capacity of 214 mg/g for the clay. SEM/EDX analysis conducted before and after adsorption corroborated the malachite green adsorption onto the clay surface. EDX spectra analysis indicated a rise in carbon intensity, underscoring the organic

nature of the malachite green dye. The examined clay emerges as a cost-effective adsorbent for removing malachite green from aqueous solutions.

References

[1] X. Jia, J. Li, E. Wang, Lighting-Up of the Dye Malachite Green with Mercury(II)–DNA and Its Application for Fluorescence Turn-Off Detection of Cysteine and Glutathione, Chem. Eur. J. 18 (2012) 13494–13500. https://doi.org/10.1002/chem.201103768

[2] H. Worku, Rethinking urban water management in Addis Ababa in the face of climate change: An urgent need to transform from traditional to sustainable system, Environmental Quality Mgmt. 27 (2017) 103–119. https://doi.org/10.1002/tqem.21512

[3] M. Amin, A. Khodabakhshi, Determination of malachite green in trout tissue and effluent water from fish farms, Int J Env Health Eng. 1 (2012) 10. https://doi.org/10.4103/2277-9183.94394

[4] J.A. Bañuelos, O. García-Rodríguez, A. El-Ghenymy, F.J. Rodríguez-Valadez, L.A. Godínez, E. Brillas, Advanced oxidation treatment of malachite green dye using a low cost carbon-felt air-diffusion cathode, Journal of Environmental Chemical Engineering. 4 (2016) 2066–2075. https://doi.org/10.1016/j.jece.2016.03.012

[5] P.O. Oladoye, T.O. Ajiboye, W.C. Wanyonyi, E.O. Omotola, M.E. Oladipo, Insights into remediation technology for malachite green wastewater treatment, Water Science and Engineering. 16 (2023) 261–270. https://doi.org/10.1016/j.wse.2023.03.002

[6] M.T.M. Hussien Hamad, Optimization study of the adsorption of malachite green removal by MgO nano-composite, nano-bentonite and fungal immobilization on active carbon using response surface methodology and kinetic study, Environ Sci Eur. 35 (2023) 26. https://doi.org/10.1186/s12302-023-00728-1

[7] T. Zhao, S. Xu, F. Hao, Differential adsorption of clay minerals: Implications for organic matter enrichment, Earth Sci Rev . 246 (2023) 104598. https://doi.org/10.1016/j.earscirev.2023.104598

[8] H. Ouallal, Y. Dehmani, H. Moussout, L. Messaoudi, M. Azrour, Kinetic, isotherm and mechanism investigations of the removal of phenols from water by raw and calcined clays, Heliyon. 5 (2019) e01616. https://doi.org/10.1016/j.heliyon.2019.e01616

[9] H. Moussout, H. Ahlafi, M. Aazza, H. Maghat, Critical of linear and nonlinear equations of pseudo-first order and pseudo-second order kinetic models, Karbala International Journal of Modern Science. 4 (2018) 244–254. https://doi.org/10.1016/j.kijoms.2018.04.001

[10] R. Ghibate, O. Senhaji, R. Taouil, Kinetic and thermodynamic approaches on Rhodamine B adsorption onto pomegranate peel, CSC EE. 3 (2021) 100078. https://doi.org/10.1016/j.cscee.2020.100078

[11] M. Aazza, H. Ahlafi, H. Moussout, H. Maghat, Adsorption of metha-nitrophenol onto alumina and HDTMA modified alumina: Kinetic, isotherm and mechanism investigations, J. Mol. Liq. 268 (2018) 587–597. https://doi.org/10.1016/j.molliq.2018.07.095

[12] H.N. Tran, Y.-F. Wang, S.-J. You, H.-P. Chao, Insights into the mechanism of cationic dye adsorption on activated charcoal: The importance of π–π interactions, *PSEP* 107 (2017) 168–180. https://doi.org/10.1016/j.psep.2017.02.010

[13] S. Iaich, Y. Miyah, F. Elazhar, S. Lagdali, M. El-Habacha, Low-cost ceramic microfiltration membranes made from Moroccan clay for domestic wastewater and Congo Red dye treatment, DWT. 235 (2021) 251–271. https://doi.org/10.5004/dwt.2021.27618

[14] M.E. Ouardi, L. Saadi, M. Waqif, H. Chehouani, I. Mrani, M. Anoua, A. Noubhani, Characterization of the bouchane phosphate (Morocco) and study of the elements of the main control elements of its calcination, Phys. Chem. News (2010).

[15] H. Ouallal, M. Azrour, M. Messaoudi, H. Moussout, L. Messaoudi, N. Tijani, Incorporation effect of olive pomace on the properties of tubular membranes, JECE . 8 (2020) 103668. https://doi.org/10.1016/j.jece.2020.103668

[16] P.S. Nayak, B.K. Singh, Instrumental characterization of clay by XRF, XRD and FTIR, Bull Mater Sci. 30 (2007) 235–238. https://doi.org/10.1007/s12034-007-0042-5

[17] M. Abewaa, A. Mengistu, T. Takele, J. Fito, T. Nkambule, Adsorptive removal of malachite green dye from aqueous solution using Rumex abyssinicus derived activated carbon, Sci Rep. 13 (2023) 14701. https://doi.org/10.1038/s41598-023-41957-x

[18] N.S. Randhawa, N.N. Das, R.K. Jana, Adsorptive remediation of Cu(II) and Cd(II) contaminated water using manganese nodule leaching residue, Desalination and Water Treatment. 52 (2014) 4197–4211. https://doi.org/10.1080/19443994.2013.801324

[19] P. Saha, S. Chowdhury, S. Gupta, I. Kumar, Insight into adsorption equilibrium, kinetics and thermodynamics of Malachite Green onto clayey soil of Indian origin, Chem. Eng. J, 165 (2010) 874–882. https://doi.org/10.1016/j.cej.2010.10.048

[20] K. Kalpana, S. Arivoli, K. Veeravelan, Activated Carbon Merremia emarginata Adsorption Capacities of Low-cost Adsorbent for Removal of Methylene Blue, Eco. Env. & Cons,. 28 (2022) S425–S430. https://doi.org/10.53550/EEC.2022.v28i08s.064